

# Dual-Drug Encapsulation and Release from Core–Shell Nanofibers

Yan Su<sup>a,b,c</sup>, Qianqian Su<sup>d</sup>, Wei Liu<sup>a,b,c</sup>, Guori Jin<sup>c</sup>, Xiumei Mo<sup>a,b,\*</sup> and Seeram Ramakrishna<sup>b,c,e</sup>

<sup>a</sup> State Key Laboratory for Modification of Chemical Fibers and Polymer Materials, Donghua University, Shanghai 201620, P. R. China

<sup>b</sup> Biomaterials and Tissue Engineering Laboratory, College of Chemistry and Chemical Engineering and Biotechnology, Donghua University, Shanghai 201620, P. R. China

<sup>c</sup> Faculty of Engineering, Department of Mechanical Engineering, National University of Singapore, 117543, Singapore

<sup>d</sup> Department of Chemistry, National University of Singapore, 117543, Singapore

<sup>e</sup> Faculty of Science, King Saud University, Riyadh 11451, Kingdom of Saudi Arabia

Received 22 December 2010; accepted 22 February 2011

## Abstract

The purpose of this work was to develop a type of tissue-engineering scaffold or drug-delivery carrier with the capability of encapsulation and controlled release of dual drugs. In this study, Rhodamine B and bovine serum albumin (BSA) were successfully incorporated into nanofibers by means of blending or coaxial electrospinning. The morphology of composite nanofibers was studied by scanning electron microscopy (SEM) and transmission electron microscopy (TEM). The composite nanofibrous mats made from coaxial electrospinning were characterized by X-ray diffraction. *In vitro* dual-drug release behaviors from composite nanofibrous mats were investigated. From the drug-release profiles, it shows that the location where the drug or protein is put into (into the core or shell of the nanofibers) can affect the drug-release profile in the coaxially electrospun fibers. The results imply that the drug- and/or protein-release profile in composite fibrous mats made from electrospinning can be controlled by altering the coaxial electrospinning process and has significant implications for a wide range of applications such as tissue regeneration, combined therapies or even cancer treatments.

© Koninklijke Brill NV, Leiden, 2012

## Keywords

Dual drug, dual protein, coaxial electrospinning, nanofibers, controlled release

## 1. Introduction

Electrospinning is a combination of two techniques, namely electro spraying and spinning [1]. In the electrospinning process, electric force is used to drive the poly-

\* To whom correspondence should be addressed. E-mail: xmm@dhu.edu.cn

mer solution(s) or melt(s) for generating nanofibers. The conventional spinning processes, including wet-, dry- and wet/dry-spinning techniques, are capable of producing fibers with diameters in the micrometer range. Unlike conventional spinning, electrospinning is capable of producing fibers with diameters ranging from tens of nanometers to micrometers [2]. Due to the ultra-thin diameter, electrospun fibers possess many extraordinary properties, for example, a large specific surface area, which makes the attachment of human cells to these fibers much easier [3, 4]. The scaffolds with nanoscale fibrous structure can absorb proteins and present more binding sites to cell membrane receptors [5, 6]. Additionally, the non-woven fibrous mats made of electrospun polymer nanofibers offer a unique capability to control the fiber diameters by adjusting applied voltage, collecting distance, solution concentration and solution flow rate [7]. Many synthetic and/or natural polymers including, but not limited to, polylactide (PLA) [8], poly( $\epsilon$ -caprolactone) (PCL) [9], poly(glycolic acid) (PGA) [10], poly(L-lactide-*co*-caprolactone) (PLLACL) [11, 12], proteins (e.g., collagen) [13, 14] and polysaccharides (e.g., chitosan) [15, 16] have been electrospun into nanofibrous mats.

Electrospun polymer nanofibers have been used for the application of drug-release systems. Because of their outstanding features, such as extremely high surface area to volume ratio [8, 17–19], electrospun nanofibers have several advantages over other dosage forms, including the drug-release profile which can be finely tailored by a modulation on the morphology, porosity and composition of the nanofiber membrane [20]; the very small diameter of the nanofibers means a short length for diffusion; and the high surface area is helpful to a mass transfer and efficient drug release. To be used as drug-delivery systems, there is particular interest in producing biodegradable nanofibers which could encapsulate and release drugs or bio-growth factors over a long period of time [21]. The drug-release characteristics depend on how well the drug is encapsulated inside the resulting nanofibers. Low efficiency of drug delivery and burst release are some of the most difficult problems. Therefore, core-shell structure nanofibers were developed to overcome the burst-release problem. Moreover, the core-shell type nanofibers can protect an unstable biological agent from aggressive environments, deliver the bioactive molecules or drugs in a sustained way, and functionalize the surface of nanostructures without affecting the core material.

In recent times, combined therapy with drugs and growth factors of different therapeutic effects show an effective way in the treatment of diseases and tissue regeneration [22, 23]. In order to optimize their effects, different drugs and growth factors should be used at optimal doses and at different periods in the treatment. One of the main challenges of combined therapy is to control the release behavior of each drug independently. However, simple drug-delivery systems cannot fulfill the needs of such therapies. Therefore, developing a dual-drug delivery system which can control the release behavior of each drug is desired. Research on dual-drug delivery systems have been reported so far. For example, Su *et al.* developed a dual-drug-loaded system by emulsion electrospinning, which simultaneously contains

drugs in the core and outer layer of the nanofibers. The resulting dual-drug-loaded nanofibers show different release profiles [24].

In the present study, two agents, bovine serum albumin (BSA) and Rhodamine B, were incorporated into PLLACL nanofibers by coaxial electrospinning. The objective of this study was to develop a type of tissue-engineering scaffold or drug-delivery carrier that is capable to encapsulate dual drug and/or protein and at the same time, allows for the ability to control and alters the drug-release profile.

## 2. Materials and Methods

### 2.1. Materials

PLLACL with a molar ratio of 75% L-lactide and 25% caprolactone was purchased from Sigma-Aldrich. 1,1,1,3,3,3-Hexafluoro-2-propanol (HFP) was purchased from Shanghai Fine Chemicals. Rhodamine B and BSA were purchased from Sigma-Aldrich. All materials and solvents were used without any further purification.

### 2.2. Preparation of Electrospinning Solutions and Electrospinning of Fibrous Mats

Solution A was prepared by dissolving 0.8 g PLLACL in 10 ml HFP, thereafter, 0.008 g Rhodamine B and 0.016 g BSA were added. The mixture was stirred at 240 rpm overnight to obtain a uniform solution. Solution B was prepared by dissolving 0.8 g PLLACL and 0.008 g Rhodamine B in 10 ml HFP as the shell solution, and the core solution was 0.016 g BSA dissolved in 10 ml distilled water. Solution C was fabricated by dissolving 0.8 g PLLACL and 0.016 g BSA in 10 ml HFP as the shell solution, and the core solution was 0.008 g Rhodamine B dissolved in 10 ml distilled water. Solution D was fabricated by dissolving BSA and Rhodamine B into distilled water to make a solution as the core solution; 0.8 g PLLACL was dissolved into 10 ml HFP as the shell solution. The details of solutions A–D are shown in Table 1.

The equipment setup comprises a syringe-like apparatus with an inner needle coaxially placed inside an outer one, as shown in Fig. 1. Two syringe pumps (Cole-Parmer Instrument) were used to push the solutions from the inner and outer

**Table 1.**  
Components of solutions for electrospinning

Solution	Shell	Core
A	PLLACL/BSA and Rhodamine B	–
B	PLLACL/Rhodamine B	BSA
C	PLLACL/BSA	Rhodamine B
D	PLLACL	BSA and Rhodamine B

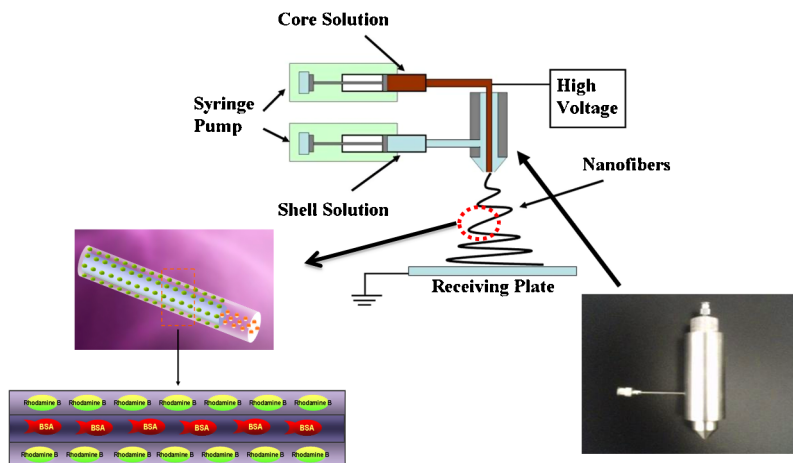


**Figure 1.** Basic setup for coaxial electrospinning. Inset: the special apparatus used in coaxial electrospinning and schematic illustration of coaxial electrospun nanofiber-loaded Rhodamine B and BSA. This figure is published in colour in the online edition of this journal, which can be accessed via <http://www.brill.nl/jbs>

needles, respectively. The inner needle has an inner diameter of 0.8 mm and an outer diameter of 1 mm; the outer needle has an inner diameter of 1.8 mm. A copper electrode connects the inner needle directly to a high voltage and the amount of electric potential transferred to the shell solution depends on the conductivity of the needle, the core and the shell solutions. An aluminum foil was connected as ground and then used to collect the fibers. The core solution was injected at a controlled flow rate of 0.20 ml/h and the shell solution at 1.0 ml/h. The distance between the needles and the collector was set to 12 cm. All of the electrospun nanofibers were obtained at ambient temperature of 22–25°C with a relative humidity of 40–60%.

### 2.3. Morphology of Fibrous Mats before and after Release

A digital vacuum scanning electron microscope (SEM; JSM-5600 LV, JEOL) was employed to examine the morphology of the prepared nanofibrous mats. Prior to SEM examination, the specimens were sputter-coated with gold to avoid charge accumulation.

Verification of the core–shell structure was conducted by transmission electron microscopy (TEM; H-800, Hitachi) at 100 kV, and the samples for TEM observations were prepared by collecting the nanofibers onto carbon-coated Cu grids.

The diameter of the electrospun ultrafine nanofibers was measured with image visualization software (Image-J 1.34, National Institutes of Health). Average fiber diameter and diameter distribution were determined by measuring about 100 random fibers from the SEM images.

## 2.4. X-Ray Diffraction (XRD) Patterns

The samples were tested using an XRD instrument (D/MAX-2550PC, Rigaku) with Cu  $K_{\alpha 1}$ , at 40 kV and 300 mA. In this work, PLLACL fibers and composite fibers with protein/drug incorporated were studied. The samples were scanned from 5 to 60° at a scanning rate of 5°/min.

## 2.5. Drug-Release Behavior Study

For the drug-release behavior study, composite fibrous mats electrospun from solutions A–D, each weighing about 50 mg, were soaked in glass vials with 100 ml PBS. The fibrous mats were incubated at 37°C in the presence of 5% CO<sub>2</sub>. At various time points, 2 ml supernatant was retrieved from the vial followed by diluting them to 10 ml using PBS, and an equal volume of fresh medium was replaced. The concentration of Rhodamine B (at an optical wavelength of 550 nm) and BSA (at an optical wavelength of 280 nm) in the supernatant were then determined by an UV-Vis spectrophotometer (WFZ UV-2102 Unique Technology Shanghai).

## 3. Results

### 3.1. Morphology of Electrospun Fibers

SEM images of dual-drug-loaded PLLACL composite nanofibers prepared under various solutions described in Section 2.2 are shown in Fig. 2. The composite nanofibers made from coaxial electrospinning (Fig. 2b–d) are uniform and smooth, with interconnected pores. The plot on the right-hand side of Fig. 2 shows the average diameters of composite electrospun nanofibers made from different solutions. Only the non-conglutinated part of the fibers was used to measure their diameters.

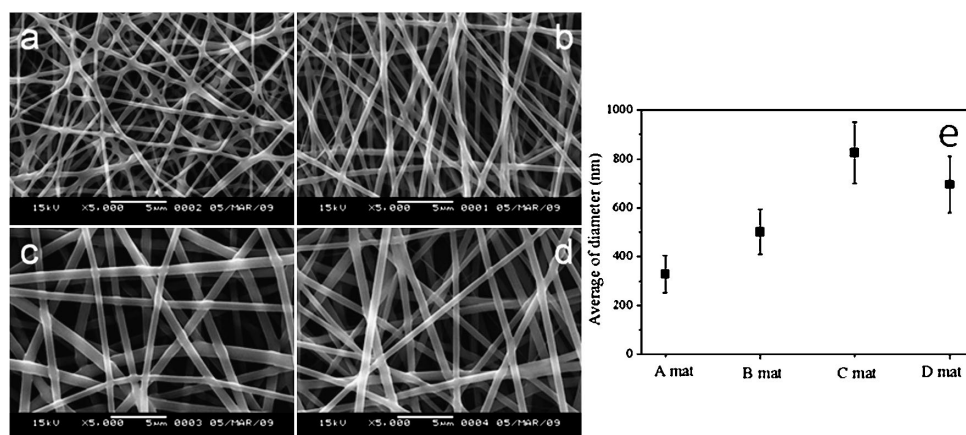


**Figure 2.** (a–d) Representative morphologies of the nanofibrous mats electrospun from solutions A–D described in Table 1. (e) Average diameters of nanofibrous mats electrospun from solution of A, B, C and D.

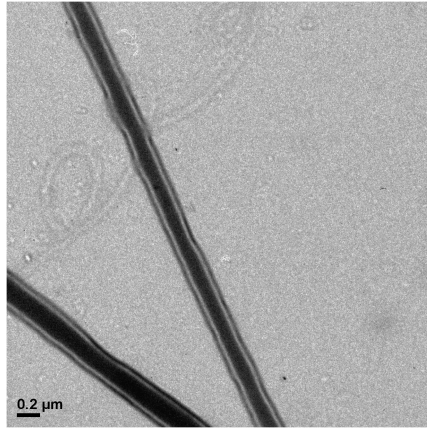


**Figure 3.** TEM micrographs of the core–shell structure, Rhodamine B was in the shell and BSA in the core of the nanofiber.

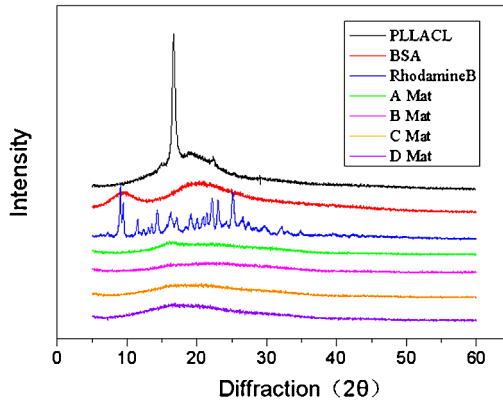


**Figure 4.** XRD patterns of PLLACL, BSA, Rhodamine B and the nanofibrous mats electrospun from solutions A–D. This figure is published in colour in the online edition of this journal, which can be accessed via <http://www.brill.nl/jbs>

From this plot, we can see that the average diameters range from 300 to 850 nm and that the average diameter using solution A has the smallest average diameter.

Figure 3 shows the TEM micrographs of the core–shell structure of PLLACL nanofibers, which Rhodamine B loaded in the shell and BSA loaded in the core of the nanofibers.

### 3.2. XRD Patterns

XRD patterns of the electrospun composite nanofibrous mats (A–D), powders of BSA and Rhodamine B, and PLLACL nanofibrous mat are displayed in Fig. 4. Electrospun PLLACL nanofibers were crystalline, showing an intensity peak at  $2\theta$  of  $16.6^\circ$  and a lower intensity at  $2\theta$  of  $22.3^\circ$ . It was also shown that Rhodamine B was crystalline, with many characteristic peaks, while BSA was amorphous,

without any characteristic peak. The crystalline Rhodamine B was not detected in any of the Rhodamine B-loaded PLLACL composite fibers because there was less than 1.0% Rhodamine B in the resultant nanofibrous mats. Drugs were molecularly dispersed within the polymer and existed in amorphous state in the composite nanofibers and there was no chemical reaction or intermolecular action between polymer and drugs.

### 3.3. In Vitro Release Study

The release behavior of BSA and Rhodamine B from composite fibrous mats was studied and the results are shown in Fig. 5. Experiments were performed in triplicate and error bars indicate the standard deviation. The release profile for electrospinning cases was studied at three stages: an initial burst release (stage I), followed by a decelerating release (stage II) and a constant release (stage III). With reference to mat A (Fig. 5a), there was an initial burst release of BSA and Rhodamine B during stage I (within 6 h) and the amount released was 53–67%. After stage I, the release curves exhibited a decelerating release rate. Between 6 and 260 h (stage II),

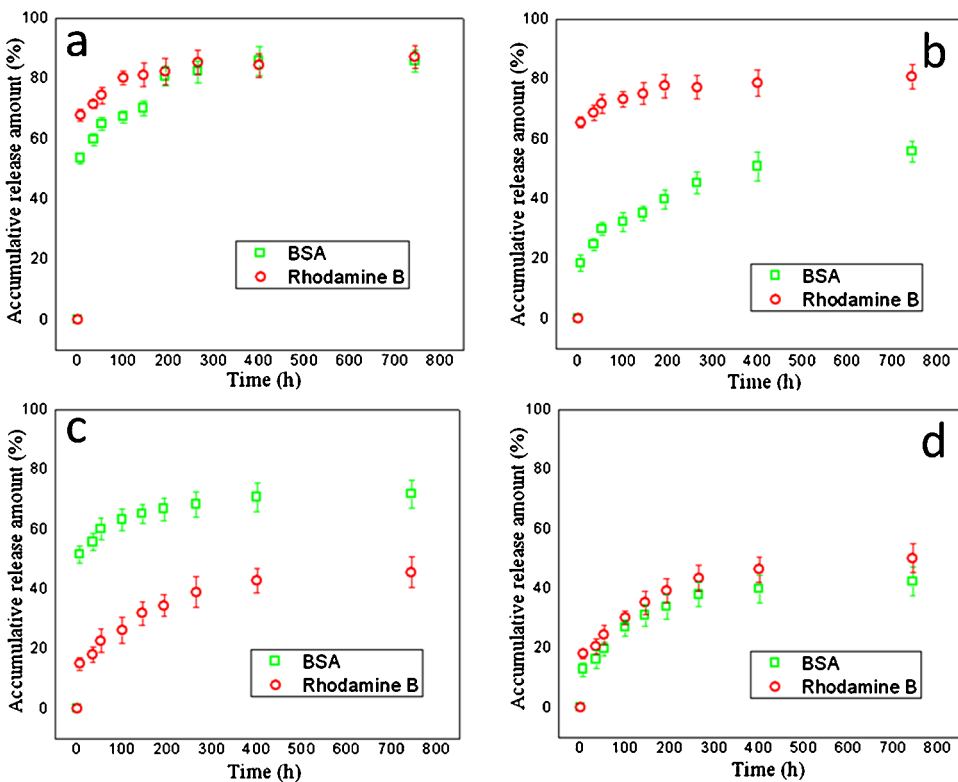


**Figure 5.** (a–d) Release profiles of BSA and Rhodamine B from mats A–D, respectively ( $T = 37^{\circ}\text{C}$ , pH 7.4). This figure is published in colour in the online edition of this journal, which can be accessed via <http://www.brill.nl/jbs>

the amount released reached 82–85%. After 260 h, the amount of drug or protein released from the blended nanofibers was at a constant rate and reached 85–87%. BSA and Rhodamine B release behavior from coaxial electrospun composite membranes (mat B) is shown in Fig. 5b. The release profile of BSA from nanofibers matrix presents a slow and steadily increasing release from the start, while Rhodamine B had a burst release at the beginning. At the end of the release study, the ultimate release percentage of Rhodamine B was about 80%, and the percentage of BSA was only 55%. Because BSA was incorporated in the core parts, and Rhodamine B was located on the shell layer of the nanofibers. Figure 5c indicates the two model drugs' release profiles from coaxial electrospun composite membranes (mat C). BSA was put into the shell and Rhodamine B was located in the core of the nanofibers in mat C. The release profile of these two drugs is similar to that of mat B. BSA has a burst and fast release, while Rhodamine B has a stable and constant release during the whole release process. In mat D, both BSA and Rhodamine B are put into core of the nanofibers and their release profiles are shown in Fig. 5d. It is seen that they present a similar release behavior. Only 12% of BSA and 18% Rhodamine B was released within first 6 h, respectively. Both BSA and Rhodamine B present a sustained release manner in the remaining 768 h.

### 3.4. Morphology of Nanofibrous Mats after Release

In this study, the degradability and morphological sustainability of the electrospun composite nanofibrous mats were also investigated after immersion in PBS for 31 days. Degradation profiles of the composite nanofibrous mats were evaluated macroscopically by SEM and shown in Fig. 6. In contrast to the smooth surface of fibers before incubation as shown in Fig. 2, visible changes of the morphologies of nanofibrous mats were observed. As shown in Fig. 6, the electrospun composite

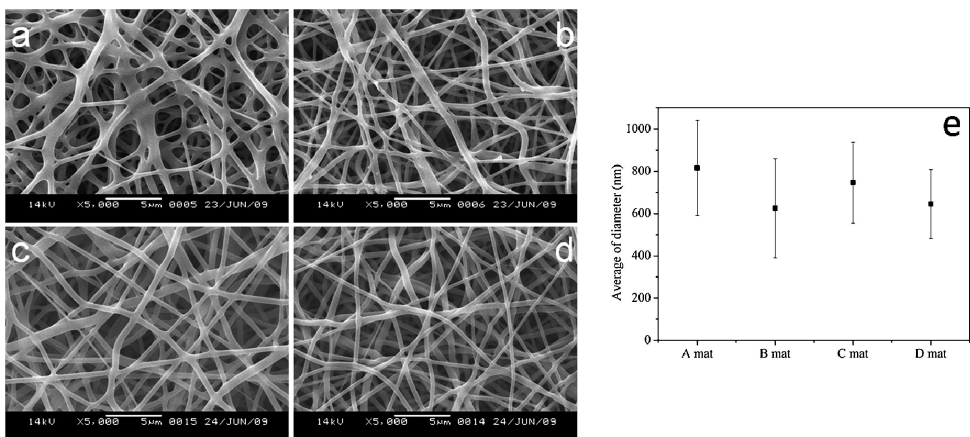


**Figure 6.** (a–d) SEM images showing representative morphologies of the nanofibrous mats electrospun from A–D after drugs release in PBS under different conditions. (e) Average diameters of nanofibrous mats after 31 days release.

nanofibrous mats almost lost their original morphology after incubation in PBS for 774 h and the degree of degradation of the nanofibrous mats were similar. The average diameter of fibrous mats after 31 days release is shown in Fig. 6e. The average diameter of mat A increased after 31 days drugs release. The other three samples did not show significant changes.

#### 4. Discussion

From the average diameter of four different nanofibers, the average diameter using solution A has the smallest average diameter. The reason is that Rhodamine B and BSA have relatively high conductivity compared to the solvent (HFP) and co-polymer (PLLACL), and it is these drugs that provide a substantial amount of charge ions. As such, the blended solution A has a higher conductivity compared to the other solutions. A higher conductivity makes the nanofibers easier to elongate and this explains why solution A produces the smallest average diameter. In the electrospinning system, there are a number of parameters that affect the fiber morphology and fiber diameter. They are polymer concentration/viscosity, applied voltage, needle diameter and the delivery rate of polymer solution [25].

The dual-drugs release mechanism is affected by two main factors. The first being diffusion and the second being degradation of the polymer. Figure 1 shows an overview of the encapsulated nanofibers, while Fig. 7 shows a schematic of drug release. From Fig. 7, it is intuitive to see that the thicker the sheath or the higher the ratio of the thickness of the shell to core, the slower the rate of diffusion of the drug through the sheath and, subsequently, the drug-release profile will be slower and steadier. As such, adjusting this ratio can affect the dual-drug release rate. Figure 6 shows that the morphology of nanofibrous mats was changed after 31 days release, but the degree of degradation was not high. Degradation may occur at the molecular level during the release process. It is indicated that the drug was released

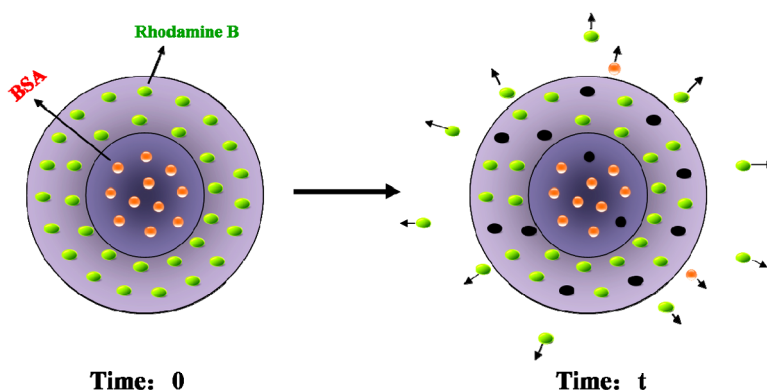


**Figure 7.** Schematic representation of the release of Rhodamine B and BSA from coaxial electrospun nanofibers. This figure is published in colour in the online edition of this journal, which can be accessed via <http://www.brill.nl/jbs>

from fibrous mats by a diffusion/erosion-coupled mechanism; however, diffusion through the pores of fibers may be the main manner.

The experimental results demonstrate that the release behavior of drugs and/or proteins can be influenced and varied by the method of electrospinning, namely, blending or coaxial electrospinning. Furthermore, the diffusion rate is affected by the ratio of the thickness of the shell to core and, as such, adjusting this ratio can affect the dual-drug release rate. When the drug and/or protein is encapsulated in the core of the nanofibers, the release profile would be slow and steady rising; however, when the drug and/or protein is put into the shell of the nanofibers, there would be a burst release in the beginning.

## 5. Conclusion

This paper presents a dual-drug loading and release system using the coaxial electrospinning method. Rhodamine B or BSA when put into the shell layer of the nanofibers shows a sharp initial burst release, while Rhodamine B or BSA when put into the core of the fiber results in a slow and steady long-term release in the coaxial electrospun fibers. The two different methods of incorporating drugs, blended and coaxial electrospinning (putting the drug in the core solution or in the shell solution) create different drug release profiles. The implication is significant because it means that the drug-release profile can be controlled and gives current drug-release applications further room for flexibility. In fact, the significance of this system is further amplified because of the wide range of drugs and or proteins that can be put into the shell or core solution and as such, signals a great potential for use in many other applications such as tissue regeneration, combined therapies or even cancer treatments.

## Acknowledgements

This research was supported by the National High Technology Research and Development Program (863 Program, 2008AA03Z305), Science and Technology Commission of Shanghai Municipality Program (08520704600 and 0852nm03400), '111 Project' Biomedical Textile Materials Science and Technology (B07024) and Shanghai Unilever Research and Development Fund (08520750100), State Key Laboratory for Modification of Chemical Fibers and Polymer Materials research program (LZ0906).

## References

1. T. Subbiah, G. S. Bhat, R. W. Tock, S. Pararneswaran and S. S. Ramkumar, *J. Appl. Polym. Sci.* **96**, 557 (2005).
2. D. H. Reneker, A. L. Yarin, E. Zussman and H. Xu, *Adv. Appl. Mech.* **41**, 43 (2007).
3. S. J. Shao, S. B. Zhou, L. Li, J. R. Li, C. Luo, J. X. Wang, X. H. Li and J. Weng, *Biomaterials* **32**, 2821 (2011).

4. A. Subramanian, U. M. Krishnan and S. Sethuraman, *J. Biomed. Sci.* **16**, 108 (2009).
5. S. Agarwal, J. H. Wendorff and A. Greiner, *Adv. Mater.* **21**, 3343 (2009).
6. W. F. Zheng, W. Zhang and X. Y. Jiang, *Adv. Eng. Mater.* **12**, 451 (2010).
7. X. Q. Li, Y. Su, R. Chen, C. L. He, H. S. Wang and X. M. Mo, *J. Appl. Polym. Sci.* **111**, 1564 (2009).
8. E. R. Kenawy, G. L. Bowlin, K. Mansfield, J. Layman, D. G. Simpson, E. H. Sanders and G. E. Wnek, *J. Control. Rel.* **81**, 57 (2002).
9. F. Chen, C. N. Lee and S. H. Teoh, *Mater. Sci. Eng. C* **27**, 325 (2007).
10. Y. You, S. W. Lee, J. H. Youk, B. M. Min, S. J. Lee and W. H. Park, *Polym. Degrad. Stabil.* **90**, 441 (2005).
11. X. M. Mo, C. Y. Xu, M. Kotaki and S. Ramakrishna, *Biomaterials* **25**, 1883 (2004).
12. F. Chen, X. Q. Li, X. M. Mo, C. L. He, H. S. Wang and Y. Ikada, *J. Biomater. Sci. Polymer Edn* **19**, 677 (2008).
13. J. A. Matthews, G. E. Wnek, D. G. Simpson and G. L. Bowlin, *Biomacromolecules* **3**, 232 (2002).
14. K. Ma, C. K. Chan, S. Liao, W. Y. Hwang, Q. Feng and S. Ramakrishna, *Biomaterials* **29**, 2096 (2008).
15. N. Bhattarai, D. Edmondson, O. Veiseh, F. A. Matsen and M. Q. Zhang, *Biomaterials* **26**, 6176 (2005).
16. Y. Z. Zhang, J. R. Venugopal, A. El-Turki, S. Ramakrishna, B. Su and C. T. Lim, *Biomaterials* **29**, 4314 (2008).
17. Y. Su, X. Q. Li, L. J. Tan, C. Huang and X. M. Mo, *Polymer* **50**, 4212 (2009).
18. S. Y. Chew, J. Wen, K. F. Yim and K. W. Leong, *Biomacromolecules* **6**, 2017 (2005).
19. Y. Su, X. Q. Li, Y. N. Liu, Q. Q. Su, M. Lim and X. M. Mo, *J. Biomater. Sci. Polymer Edn* **22**, 165 (2011).
20. N. Ashammakhi, A. Ndreu, A. M. Piras, L. Nikkola, T. Sindelar and H. Ylikauppila, *J. Nanosci. Nanotechnol.* **7**, 862 (2007).
21. H. H. Huang, C. L. He, H. S. Wang and X. M. Mo, *J. Biomed. Mater. Res. A* **90**, 1243 (2009).
22. L. Y. Qiu and Y. H. Bae, *Biomaterials* **28**, 4132 (2007).
23. J. S. Lee, J. W. Bae, Y. K. Joung, S. J. Lee, D. K. Han and K. D. Park, *Int. J. Pharm.* **346**, 57 (2008).
24. Y. Su, X. Q. Li, S. P. Liu, X. M. Mo and S. Ramakrishna, *Colloid Surfaces B* **73**, 376 (2009).
25. Q. P. Pham, U. Sharma and A. G. Mikos, *Tissue Eng.* **12**, 1197 (2006).